

Article

Operator-Based Adaptive Tracking Capacity Control in Complex Manufacturing Processes

Ping Liu ^{1,*} , Qiang Zhang ², Aihui Wang ³ , Shengjun Wen ¹ and Jürgen Pannek ⁴¹ Zhongyuan-Petersburg Aviation College, Zhongyuan University of Technology, Zhengzhou 451191, China² School of Intelligent Engineering, Zhengzhou University of Aeronautics, Zhengzhou 450015, China³ School of Electronic and Information, Zhongyuan University of Technology, Zhengzhou 451191, China⁴ Faculty of Mechanical Engineering, Technische Universität Braunschweig, 38106 Braunschweig, Germany

* Correspondence: pingliu@zut.edu.cn

Abstract: Nowadays, quickly changing customer demands are a big challenge in the manufacturing industry, especially for job shops, which are typical coupling and nonlinear multi-input–multi-output (MIMO) systems. In order to achieve good shop floor performance in the presence of short-term demand fluctuations, a key performance indicator—work in process (WIP)—is required to be effectively controlled in the vicinity of the desired levels. For this purpose, a machinery-oriented capacity adjustment approach via a reconfigurable machine tool (RMT) is employed to flexibly balance capacity and load in the case of a bottleneck. A mathematical model concerning the RMT and WIP was first established in the presence of uncertainty and delays. The operator-based robust right coprime factorization (RRCF) method was adopted to stabilize the uncertain system, and adaptive integral separated proportional–integral (ISPI) tracking controllers were further designed to improve the transient and robustness performance. The performance of the proposed ISPI-RRCF was analyzed and compared with that of a state-of-the-art method in a simulation. The results showed that both control systems could ensure that the WIP was within an allowed bound, while the former had lower overshoots, shorter setting times, and more concentrated distributions facing stochastic demands. This further indicated the effectiveness of the proposed algorithm in the avoidance of serious bottlenecks and unbalanced capacity distributions.

Keywords: operator theory; adaptive tracking capacity control; job shop; reconfigurable machine tool

Citation: Liu, P.; Zhang, Q.; Wang, A.; Wen, S.; Pannek, J. Operator-Based Adaptive Tracking Capacity Control in Complex Manufacturing Processes. *Appl. Sci.* **2023**, *13*, 449. <https://doi.org/10.3390/app13010449>

Academic Editor: Dimitris Mourtzis

Received: 2 December 2022

Revised: 19 December 2022

Accepted: 23 December 2022

Published: 29 December 2022



Copyright: © 2022 by the authors. Licensee MDPI, Basel, Switzerland. This article is an open access article distributed under the terms and conditions of the Creative Commons Attribution (CC BY) license (<https://creativecommons.org/licenses/by/4.0/>).

1. Introduction

With rapidly changing customer demand, along with the requirements of cost-effectiveness, high customization, and short delivery time, manufacturing processes have become more complex and dynamic [1,2]. Job shops are a typical flexible production mode for producing a variety of products with small lot sizes. However, they suffer from a high work-in-process (WIP) level, high costs, long lead times, and low productivity, which may lead to bottlenecks and cause performance deterioration [3,4]. To cope with these challenges and achieve good shop-floor performance in a job shop environment, as an effective supporting tool for compensating and balancing the capacity distribution, capacity adjustments are conducted on the operational layer. In [5], a decentralized capacity control structure was designed to deal with bottlenecks for the capacity balance between workstations in job shop systems. In [6], an improved centralized model predictive control (MPC) algorithm was proposed to optimize capacity adjustment processes to avoid serious bottlenecks. A local capacity adjustment was discussed based on the H_∞ algorithm to ensure that the WIP was in the vicinity of a planned level in [7]. These studies show that capacity adjustment is an effective way to improve performance, even with small modifications during a high load period. Instead of labor-oriented approaches (e.g., overtime), a reconfigurable machine tool (RMT) can be promoted as a new opportunity for a machinery-oriented capacity adjustment [8].

In [9], a harmonizing throughput–time capacity adjustment approach via an RMT was proposed to improve productivity while maintaining a certain flexibility in complex job shops. In [10], the WIP of workstations was also controlled by utilizing the flexibility of RMTs in the capacity adjustment of complex manufacturing processes.

Although RMTs play a vital role in terms of flexibility and reconfigurability, they are only an enabler for capacity adjustment. Therefore, an effective control method for the usage of RMTs is of crucial importance in the context of Industry 4.0 [11]. Due to its simplicity and wide applicability, the proportional–integral–derivative (PID) algorithm has been applied for single-input–single-output (SISO) systems. Kim and Duffie first adopted the PI algorithm in the backlog control of a single-workstation production system [12]. They further extended the application to the capacity control of a multi-workstation production system with disturbances [13]. In [14], the development of a PID method was discussed with respect to its incorporation with other advanced algorithms in practical applications, and the challenges in design and tuning for difficult problems, especially for systems with nonlinearities, coupling, disturbances, and delays (e.g., in a job shop), were also put forward.

In contrast to the PID, operator-based robust right coprime factorization (RRCF) is an advanced control method for a class of nonlinear systems that can be appropriately decomposed by using operator theory to design robust controllers via Bezout identity [15]. Deng proposed a new condition for the robust controller design of nonlinear systems with unknown bounded disturbances, which extended the application [16]. Improved RRCF algorithms were proposed to deal with delays, disturbances, and couplings [17,18]. This method was mathematically demonstrated and applied for a variety of fields, such as a highly nonlinear ionic polymer metal composite with hysteresis [19], a multi-joint manipulator [20], and a coupling multi-tank process [21], which was readily applicable for job shop systems for capacity control via RMTs. In previous work, this method was applied in capacity control. However, the performance still needs to be improved, especially for adaptive tracking control. To improve the tracking performance, a feedback-linearization-based PID method was proposed for the path tracking of micro-actuators to reduce the tracking error in [22]. Salehi Kolahi et al. designed a non-singular fast terminal sliding-mode control for the path tracking of nonlinear second-order systems with compound disturbances in [23]. For adaptive control, a neural network (NN) is an effective method. Nguyen et al. recommended an adaptive robust position control technique by integrating an radial basis function NN (RBF-NN) and NN-based disturbance observer for disturbed electro-hydraulic servo systems [24]. Ruan et al. also proposed an RBF-NN adaptive sliding-mode controller for nonlinear electromechanical actuator systems with uncertainty and disturbances [25].

Considering the key performance of job shops, WIP is essential, as it greatly influences many key performance indicators, e.g., energy efficiency, throughput, and delivery date reliability [26,27]. Hence, the purpose of control is to guarantee that the manufacturing process works on an expected WIP level via flexible capacity control with RMTs and to ensure the closed-loop stability in which the performance indicators (e.g., WIP) remain bounded while converging toward desired values or an acceptable stability region. In [28], the authors investigated the problem of WIP regulation via RMT assignment in a job shop with a constant flow probability. Desirable control performance and the stability of the closed-loop system were achieved by using MPC with terminal endpoint constraints. However, the preferred assignment of RMTs for capacity adjustment belonged to a continuous optimization case. To solve this problem, the authors further extended their work and employed MPC in association with a deterministic method (e.g., branch and bound) and stochastic optimization techniques (e.g., genetic algorithm) for the integer assignment of RMTs [29]. However, transportation delays were not taken into consideration, and the computational complexity of this method was very high due to the iterative online optimization. In [30], the complexity of workstations was described as a nonlinear operator, and the WIP was controlled by considering the productivity and customer requirements.

This also indicated the applicability of operator theory in the capacity control process. To measure the control performance, transient and robustness were two key factors facing stochastic customer demands. As a key transient performance indicator, overshoot reflects the bottleneck level of workstations and the capacity distribution; therefore, it is expected to have a low value.

The above survey revealed that the integration of RMTs and RRCCF was an effective means of capacity control. However, there is still much work to be done to improve the performance in capacity control systems while considering practical applications. This research is concerned with quickly solving the serious bottleneck represented by the high overshoot and unbalanced capacity reflected by the robustness in job shops facing stochastic demands. To solve this problem, an improved adaptive tracking capacity control algorithm is proposed by integrating the RRCCF and ISPI with a single-neuron algorithm. The main contribution can be summarized as follows:

- To decrease the complexity of a high-coupling job shop manufacturing process and autonomously realize rapid responsiveness among workstations, a decoupling-controller-based operator was designed to decompose the complex MIMO system into multiple SISO systems.
- To ensure the steady-state performance and keep the WIP level for each workstation in the vicinity of the planned values while considering disturbances and delays, robust controllers were theoretically designed by using the RRCCF method based on the Bezout identity.
- To effectively decrease the overshoot and excessive adjusting time in the face of large deviations, integral separated PI-type tracking controllers based on the RRCCF (ISPI-RRCCF) for the decomposed SISO systems were designed to improve the transient performance.
- To adaptively adjust the parameters of the ISPI-RRCCF tracking controllers and enhance the performance in real time, a single neuron associated with the supervised Hebb learning algorithm was adopted, where the related weight coefficients were constantly updated in the presence of disturbances and delays.

The remainder of this paper is structured as follows: Firstly, a mathematical model concerning job shop systems with RMTs is introduced in Section 2. Thereafter, Section 3 introduces the adaptive capacity controller design process based on operator theory. Later on, Section 4 discusses the implementation of the proposed adaptive tracking capacity control method in a simulation, and then the results are analyzed and compared with those of a previous method. Finally, this paper is concluded in Section 5.

2. Mathematical Model

In the process of adaptive capacity controller design for a job shop, a mathematical model is an important factor for the controller's design. In this section, a funnel-based development model is discussed, and it integrates the customized flexibility of RMTs within complex manufacturing processes [29,30]. In this model, the performance indicators considered are the input rate, output rate, and WIP level; these are not of interest for any single events or orders in the time domain. A general job shop manufacturing system, which consists of n workstations, is shown in Figure 1 [5]. The parameters and variables in the mathematical model of this system are shown in Table 1.

Due to the multiple parallel production paths of multiple products, the WIP levels of all workstations are generally higher than those in flow shop processes. Therefore, all machine tools are assumed to be working at the maximum productivity; then, the orders of the output rates of each workstation can be assumed to be the sum of all machines' capacities. Taking DMTs' high productivity into account, the capacity of a workstation includes the customizable part of DMTs and the changeable part of RMTs. This is given by

$$\bar{c}_i(t) = n_i^D \cdot v_i^D + n_i^R \cdot v_i^R. \quad (1)$$

Table 1. Variables within a job shop system with RMTs.

Variable	Description
$X_{ji}^I(t)$	Order input rate from the j th to the i th workstation for $j, i \in \{1, \dots, n\}$
$X_i^I(t)$	Order input rate in the i th workstation for $i \in \{1, \dots, n\}$
$X_{ij}^O(t)$	Order output rate from the i th to j th workstation for $i, j \in \{1, \dots, n\}$
$X_i^O(t)$	Order output rate in i th workstation for $i \in \{1, \dots, n\}$
p_{ij}	Order flow possibility from the i th to the j th workstation for $i, j \in \{0, \dots, n\}$
p_{i0}	Order flow possibility from the i th workstation to final stage for $i \in \{1, \dots, n\}$
p_{0i}	Order flow possibility from an initial stage to the i th workstation for $i \in \{1, \dots, n\}$
n^R	Number of RMTs in the system
n_i^D	Number of DMTs in the i th workstation for $i \in \{1, \dots, n\}$
v_i^D	Order output rate of DMTs in the i th workstation for $i \in \{1, \dots, n\}$
v_i^R	Order output rate of RMTs in the i th workstation for $i \in \{1, \dots, n\}$
$X_i^D(t)$	Disturbances in the i th workstation for $i \in \{1, \dots, n\}$
$u_i(t)$	Number of RMTs in the i th workstation $i \in \{1, \dots, n\}$
$y_i(t)$	WIP level in the i th workstation $i \in \{1, \dots, n\}$
τ_1	Transportation delay between workstations in $X_i^I(t)$
τ_2	Reconfiguration delay of RMTs in $u_i(t)$

If the number of RMTs is considered as a single input, then the output rate of the i th workstation is approximately equal to the capacity, which could be adjusted by the assigned number of RMTs. Then, the output rate is represented by

$$X_i^O(t) = n_i^D \cdot v_i^D + u_i(t) \cdot v_i^R. \tag{2}$$

As one of the key performance indicators, WIP has a great influence on productivity, delivery date, throughput, and cost. Therefore, the purpose of a capacity adjustment is to guarantee that every workstation works on an expected WIP level. Then, the WIP of each workstation can be described as the output signal of the model given by

$$y_i(t) = y_i(0) + \int_0^t X_i^I(\tau) - (n_i^D \cdot v_i^D + u_i(\tau) \cdot v_i^R) d\tau. \tag{3}$$

However, customers' demands are volatile, and delays, including transportation delays between workstations and reconfiguration delays of RMTs, always exist; cf. Figure 1. Considering these factors, the mathematical model can be represented by

$$\begin{aligned}
 y_i(t) = & y_i(0) + \int_0^t X_{0i}^I(\tau - \tau_1) + X_i^D(\tau) \\
 & + \sum_{j=1}^n p_{ji} \cdot (n_j^D \cdot v_j^D + u_j(\tau - \tau_2 - \tau_1) \cdot v_j^R) \\
 & - (n_i^D \cdot v_i^D + u_i(\tau - \tau_2) \cdot v_i^R) d\tau,
 \end{aligned} \tag{4}$$

where the transportation time τ_1 is constant in this paper, and the reconfiguration delay τ_2 is δ when RMT changes its operation from one to another workstation, but it only exists in the object, not in the original one. Thus, the reconfiguration delay is asynchronous and can be represented by

$$\tau_2 = \begin{cases} \delta, & u_i(t^+) \geq u_i(t^-), \\ 0, & \text{else.} \end{cases} \tag{5}$$

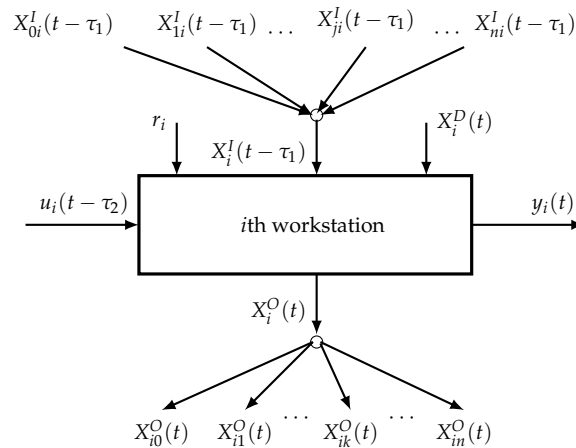


Figure 1. The general model structure of the n -workstation job shop system [31].

Furthermore, though the machine tools are assumed to be working at the maximum production rate, the capacity of the whole system is limited, and it depends on the number of RMTs in the job shop. For a job shop with n workstations and n^R RMTs, the number of RMTs at the j th workstation $u_j(t)$ is a non-negative integer, which can be described with following constraints:

$$u_i(t) \in \mathbb{N}_0 \quad \text{and} \quad \sum_{i=1}^n u_i(t) \leq n^R. \tag{6}$$

For these constraints, the truncation $\lfloor \cdot \rfloor$ and fractional approach [5] are utilized with

$$\hat{u}_i(t) = \begin{cases} \lfloor u_i(t) \rfloor, & \text{if } \sum_{i=1}^n u_i(t) \leq n^R \\ \left\lfloor \frac{n^R}{\sum_{j=1}^n u_j(t)} u_i(t) \right\rfloor, & \text{else.} \end{cases}$$

Therefore, when the sum of the RMTs exceeds n^R , $\hat{u}_i(t)$ is obtained with the fractional discrete value. Otherwise, the truncated value $u_i(t)$ is chosen.

3. Operator-Based Adaptive Capacity Control

For the capacity controller design, an improved operator-based adaptive capacity control method is proposed. Within this method, the multi-workstation job shop system is firstly decoupled into a set number of SISO systems. Thereafter, a local controller of the decoupled SISO system is designed based on operator theory, where an ISPI tracking controller is proposed according to the RRCF (ISPI-RRCF) method, and a neuron algorithm is used to optimize the parameters of the ISPI-RRCF controller. In this section, the content includes the mathematical preliminaries of operator theory, the decoupling control of the MIMO system, and the local adaptive capacity control of the decoupled SISO systems.

3.1. Mathematical Preliminaries

In operator theory, a job shop manufacturing system can be represented by an operator Q , which is a mapping from the input space U to the output space Y . The domain and range of Q are defined with $\mathcal{D}(Q)$ and $\mathcal{R}(Q)$, respectively. $\mathcal{N}(U, Y)$ donates the set of all nonlinear operators, and the Lipschitz semi-norm of Q on $\mathcal{N}(D_s, Y)$ is defined via

$$\|Q\| := \sup_{x, \tilde{x} \in D_s \& x \neq \tilde{x}} \frac{\|Q(x) - Q(\tilde{x})\|_Y}{\|x - \tilde{x}\|_U}.$$

For such complex job shop systems, the purpose is to design an adaptive capacity controller to guarantee that the job shop works at a predefined level. When the seminorm is finite, the system is called finite-gain input–output stable (simply called ‘stable’). The operator-based definitions and theorems are given as follows; cf. [5] for details.

Definition 1. Consider a causal and stabilizable operator $Q : \mathcal{D}(Q) \rightarrow \mathcal{R}(Q)$. It has the right factorization $Q = N \circ D^{-1}$, where N is causal and stable, while D is causal, stable, and invertible. Then, the right coprime factorization (RCF) of Q , which is shown in Figure 2, is defined based on the Bezout identity:

$$R \circ N + S \circ D = M, \tag{7}$$

where $R : \mathcal{R}(N) \rightarrow \mathcal{D}(Q)$ and $S : \mathcal{R}(D) \rightarrow \mathcal{D}(Q)$ are causal and stable, and $M : \mathcal{D}(Q) \rightarrow \mathcal{D}(Q)$ is a unimodular operator.

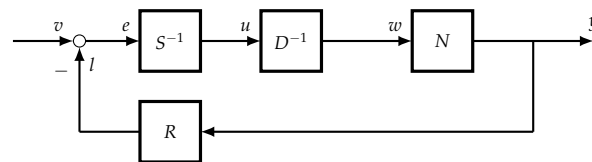


Figure 2. The right coprime factorization for an SISO system.

As shown in Figure 2, except for the input signal u and the output signal y , there exists a quasi-state signal w from the right factorization. v and l are the referred and feedback signals, and e is the error. With this definition, the dynamics of this control system can be described with the following theorem [5].

Theorem 1. Consider a causal and stabilizable operator $Q : \mathcal{D}(Q) \rightarrow \mathcal{R}(Q)$. If it has RCF, then this system is stable and can be equivalent to $y = N \circ M^{-1}(v)$.

When considering bounded uncertainties or disturbances, if the above system Q still has the right factorization with

$$Q = (N + \Delta N) \circ D^{-1} \tag{8}$$

where ΔN is an unknown bounded operator, then the following definition is given.

Definition 2. Consider a bounded disturbed system Q (8). If there exist two operators R and S satisfying the Bezout identity $R \circ (N + \Delta N) + S \circ D = \tilde{M}$, then, the system has robust right coprime factorization (RRCF), as shown in Figure 3, where \tilde{M} is also a unimodular operator.

Similarly to the Theorem 1, the RRCF of the disturbed system can be equivalent to $y = (N + \Delta N) \circ \tilde{M}^{-1}(v)$. These definitions provide an effective tool for the control and analysis of a class of nonlinear systems, especially for complex dynamic job shops. The details of the controller design process are introduced in the following; these include the decoupling controller design for MIMO systems and the local adaptive capacity control of SISO systems.

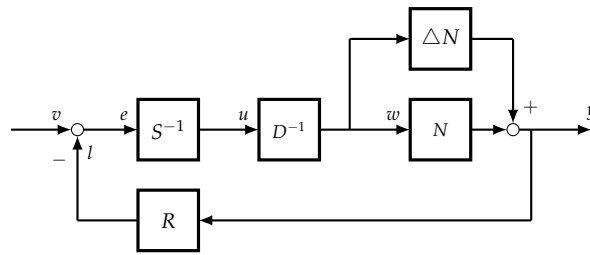


Figure 3. Nonlinear feedback system with disturbances.

3.2. Decoupling Control for MIMO Systems

A multi-workstation, multi-product job shop manufacturing process is a typical MIMO system with various delays, uncertainties, and couplings. From the definitions in Section 3.1, RRCF was adopted in the capacity control of this system. Based on the mathematical model in (4), the input rate from the initial stage $X_{0i}^I(t)$ was assumed to randomly change with a Gaussian distribution, which was considered the uncertainty of the system. The disturbance $X_i^D(t)$, e.g., the rush order, which was also from the initial stage, was included in the uncertainty $X_i^D(t)$, which was represented by ΔN_i . Then, the right factorization of the complex MIMO system was $Q = (N + \Delta N) \circ D^{-1}$, where the N and D were designed with

$$\begin{aligned}
 w_i(t) &= D_i^{-1}(u_j(t - \tau_2 - \tau_1))(u_i(t - \tau_2)) \\
 &= X_{0i}^I(t - \tau_1) + \sum_{j=1}^n p_{ji} \cdot (n_j^D \cdot v_j^D + u_j(t - \tau_2 - \tau_1) \cdot v_j^R) \\
 &\quad - (n_i^D \cdot v_i^D + u_i(t - \tau_2) \cdot v_i^R)
 \end{aligned} \tag{9}$$

$$y_i(t) = N_i + \Delta N_i = y_i(0) + \int_0^t w_i(\tau) + X_i^D(\tau) d\tau. \tag{10}$$

In (9), there are couplings among the input signals u_i for $i \in \{1, \dots, n\}$, which can be described as n linear equations. The solution is obtained with $u_i(\cdot) = \sum_{j=1}^n D_{ij}(w_j)(\cdot)$. In order to simplify the computation for the RRCF-based capacity control of the MIMO system, the following theorem is given for the decoupling controller design [5].

Theorem 2. Consider the decoupling control system shown in Figure 4. If there exists a linear operator G and a stable and invertible operator Z with

$$\sum_{j=1, j \neq i}^n [Z_{ij}(w_i)](w_j) + G_i \circ D_{ij}(w_j) = 0 \tag{11}$$

$$Z_{ii}(w_i) + G_i \circ D_{ii}(w_i) = L_i(w_i) \tag{12}$$

to ensure that L_i is stable and invertible, then the MIMO system is decoupled, where $L = (L_1, \dots, L_n)$ is the decoupled operator with $v_i = L_i(w_i)$.

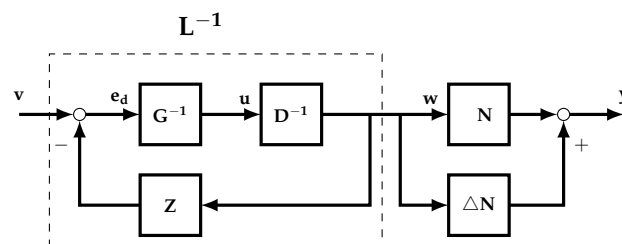


Figure 4. Decoupling structure of the MIMO system.

With this theorem, the stability of the decoupled job shop system can be proved based on the following proposition (cf. Proposition 1 in [5] for a detailed proof).

Proposition 1. Consider the system (4). Let the decoupling parameters h_i be finite with $|h_i| \neq \frac{1}{v_i^R}$, let $\mathbf{G} = (G_1, \dots, G_n)$ be the identity operator, and let Z_{ij} be unimodular for $i = 1, \dots, n$, such that

$$\sum_{j=1, j \neq i}^n [Z_{ij}(w_i)](w_j) = - \sum_{j=1, j \neq i}^n G_i \circ D_{ij}(w_j),$$

holds; then,

$$L_i(w_i) = (h_i - \frac{1}{v_i^R}) \cdot w_i - \frac{v_i^D n_i^D}{v_i^R} \tag{13}$$

holds. Furthermore, $L_i(w_i)$ is stable and invertible if n^R is sufficiently large.

3.3. Local Adaptive Capacity Control

The above decoupling controller transformed the MIMO system into n independent SISO systems. Then, while considering each decoupled SISO system, the local adaptive capacity controller is designed in two parts, namely, the RRCF controller and adaptive tracking controller for the robustness and tracking performance, respectively.

For the decoupled SISO system, the RRCF operators R_i and S_i are designed with the Bezout identity: $R_i \circ (N_i + \Delta N_i) + S_i \circ L_i = \bar{M}_i$. Then, the following theorem is presented.

Theorem 3. Consider the MIMO system (4) with the decoupling controller in Proposition 1. If the i th workstation has its local RRCF controller,

$$R_i(s(\cdot)) = (1 - K_i) \cdot s(\cdot)' \tag{14}$$

$$S_i^{-1}(s(\cdot)) = \frac{(h_i v_i^R - 1)s(\cdot)}{v_i^R K_i} - \frac{v_i^D n_i^D}{v_i^R}. \tag{15}$$

for $i = 1, 2, \dots, n$, and the RRCF control parameter $K_i \in (0, 1)$, then the feedback control system shown in Figure 5 is stable.

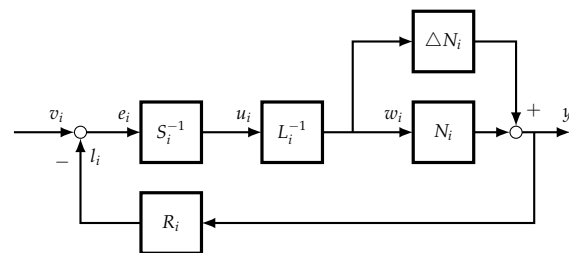


Figure 5. RRCF control of the decoupled MIMO systems.

Proof. The coupling system (4) can be represented with $y_i(t) = N_i L_i^{-1}$ for $i = 1, 2, \dots, n$ by using Proposition 1. According to the definition of RRCF 2, let

$$L_i^{-1}(s(\cdot)) = \frac{s(\cdot)v_i^R + v_i^D n_i^D}{h_i v_i^R - 1} \tag{16}$$

$$(N_i + \Delta N_i)(s(\cdot)) = \int (s(\cdot)) dt. \tag{17}$$

Additionally, according to Theorem 1, the control system can be equivalent, and its Lipschitz semi-norm is

$$\|N_i + \Delta N_i\| := \sup_{s, \bar{s} \in D_s \& s \neq \bar{s}} \frac{\|(N_i + \Delta N_i)(s) - (N_i + \Delta N_i)(\bar{s})\|_{Y_s}}{\|s - \bar{s}\|_{U_s}} < 1 + |X^D(t)|. \tag{18}$$

Because the uncertainty $X_i^D(t)$ is bounded, the Lipschitz semi-norm $\|(N_i + \Delta N_i)\|$ is finite. Finally, this can prove that the above local RRCF control system is stable. \square

Based on the RRCF controller designed for robust stability, a PI-type tracking controller (PI-RRCF), as proposed in [16], was investigated. Though integration could eliminate static differences and improve control accuracy, it may cause a large deviation in the system output during the start-up or in face of significant changes with respect to the set value, which would lead to the accumulation of integrations with the resulting overshoot or oscillation [32]. To solve these problems, therefore, an integral-separation PI tracking controller is proposed, which is called ISPI-RRCF algorithm; cf. Figure 6 for a sketch. Then, the tracking controller C_i in the j th workstation is designed as

$$C_i(s(\cdot)) = C_i^0 \cdot s(\cdot) + \beta \cdot C_i^1 \cdot \int s(\cdot) \tag{19}$$

where C_i^0 and C_i^1 are tracking parameters, β is the integral term selector switch coefficient, and ϵ is the threshold, i.e.,

$$\beta = \begin{cases} 0 & |s(\cdot)| > \epsilon \\ 1 & |s(\cdot)| \leq \epsilon \end{cases} \tag{20}$$

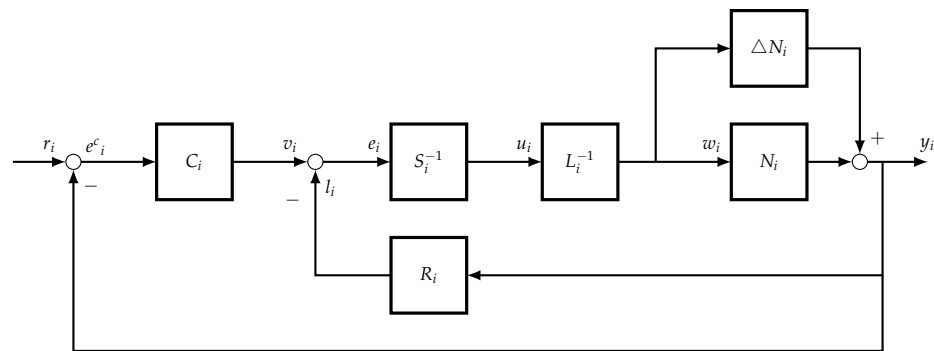


Figure 6. Nonlinear feedback tracking control of the MIMO system.

From (19) and (20), it can be seen that the integration does not work in the case of overshoot when the deviation exceeds the given threshold, and conversely, the integration would be (re-)introduced to minimize the static error once the deviation falls into the threshold. Now, the ISPI-RRCF feedback tracking control system is discussed with the following theorem.

Theorem 4. Given the bounded and disturbed MIMO system (4) and the tracking operator C_i in (19), the closed-loop system in Figure 6 is stable.

Proof. When the system is at the initial zero state, as shown in Figure 6, it obtains $y_i = (N_i + \Delta N_i)C_i(e_i^c(\cdot))$ with

$$\begin{aligned} y_i(t) &= \int C_i^0(e_i^c)(t) + \beta C_i^1 \int (e_i^c)(\tau) d\tau dt + \int C_i^0(X_i^D)(t) + \beta C_i^1 \int (X_i^D)(\tau) d\tau dt \\ &= \int C_i^0(r_i - y_i)(t) + \beta C_i^1 \int (r_i - y_i)(\tau) d\tau dt + \int C_i^0(X_i^D)(t) + \beta C_i^1 \int (X_i^D)(\tau) d\tau dt. \end{aligned} \tag{21}$$

By calculating the Laplace transformation of (21), it can be represented with

$$\hat{Q} : Y_i(s) = \frac{C_i^0 s + \beta C_i^1}{s^2 + C_i^0 s + \beta C_i^1} \cdot (R_i(s) + D_i(s)).$$

Let $S_i(\cdot) = R_i(\cdot) + D_i(\cdot)$; then, the Lipschitz semi-norm is obtained via

$$\begin{aligned} \|\hat{Q}\| &:= \sup_{F \in (0, \infty)} \sup_{S \neq \hat{S}} \frac{\|[\hat{Q}(S)]_F - [\hat{Q}(\hat{S})]_F\|}{\|[S]_F - [\hat{S}]_F\|} \\ &= \sup_{F \in (0, \infty)} \left| \frac{C_i^0 s + \beta C_i^1}{s^2 + C_i^0 s + \beta C_i^1} \right| \leq 1. \end{aligned} \tag{22}$$

Hence, the above feedback tracking control system is stable. \square

To improve the tracking control performance in complex dynamic environments, the parameters of the PI-type control are usually adaptively tuned by metaheuristic algorithms [33]. In this paper, an artificial neural network (ANN) method was considered, and a single neuron was utilized to adaptively adjust the parameters of the tracking controllers [34] (i.e., C_i^0, C_i^1 in (19)). In this case, the inputs of the single neuron were defined as $x_{i0} = e_i^c - e_i^{cp}$ and $x_{i1} = e_i^c = r_i - y_i, i = 1, \dots, n$, where e_i^c is the error between the desired and current feedback of the system, and e_i^{cp} represents the previous error. By using the connection weights of x_{ij} in the single neuron, the relationship between the input x_{ij} and the i th output v_i in the context of incremental PI control is given as

$$v_i = v_i^p + K_i \sum_{j=0}^1 \hat{w}_{ij} x_{ij}^T \quad \hat{w}_{ij} = w_{ij} / \left| \sum_{j=0}^1 w_{ij} \right| \tag{23}$$

where w_{ij} is a weighting coefficient, and $K_i > 0$ is the proportional coefficient of the neuron. Concerning the self-adaptive learning rules, the supervised Hebb learning algorithm was adopted; this included the learning rate $\xi_{ij} > 0$ and the correlative functions of input x_{ij} , output v_i , and output error e_i^c of the neuron, i.e.,

$$w_{ij} := w_{ij} + \xi_{ij} e_i^c v_i x_{ij}^T \tag{24}$$

With the update of the w_{ij} iteration, the parameters of the tracking controllers $C_{ij}, j = 0, 1$ for all workstations would be changed, and satisfactory tracking performance could be guaranteed in the presence of disturbances and delays.

Overall, the adaptive integral separation PI combined with the RRCF (ISPI-RRCF) method for WIP tracking control via RMTs is outlined in Algorithm 1.

Algorithm 1 Framework of the adaptive ISPI-RRCF

Require: Given the MIMO system with disturbances $\mathbf{Q} = (\mathbf{N} + \Delta\mathbf{N}) \circ \mathbf{D}^{-1}$;

- 1: Transfer the MIMO system into a set number of SISO systems via decoupling controllers \mathbf{Z} and \mathbf{G} ;
- 2: Design RRCF controllers \mathbf{R} and \mathbf{S} for each decoupled SISO system (workstation) to guarantee stability in the presence of uncertainty and delays.
- 3: Adopt ISPI controllers \mathbf{C} for WIP tracking while decreasing overshoot;
- 4: Optimize the parameters of the \mathbf{C} -based single neuron to improve the transient and robustness performance;

Ensure: Converged WIP level (output) for each workstation within a given prescribed threshold through the assignment of RMTs (input).

4. Numerical Simulation

In this paper, a job shop manufacturing process with four workstations and $n^R = 10$ RMTs for three products [31] is considered. The flow probabilities between the workstations were dynamically changed with volatile demands for three different types of products. The system settings and simulation results are given below.

4.1. Simulation Settings

The demands for the products were bounded and normally distributed in the form of the *randi*([45,56]) function, which was the uncertainty of the system. In terms of parameter adjustments on the tracking controllers, the initial values of the weight and learning rate of the single neuron were identical for both the PI-RRCF and ISPI-RRCF control systems. The threshold in the ISPI-RRCF system was set to $\epsilon = [90\ 90\ 90\ 90]$. The practical stability region concerning the converged WIP level was set to $\pm 3 * v_j^{RMT}$. The reconfiguration delay of the RMTs was 2 h, and the transportation delay between each workstation was 1 h. With these settings, together with those in Table 2, a performance analysis and a comparison of both control systems are given in the following.

Table 2. Simulation settings of the case study [35].

Workstation	1	2	3	4
Initial WIP level	400	400	300	200
Referred WIP level	240	400	400	240
Number of DMTs	4	2	2	4
Output rate of DMTs	20	40	40	20
Output rate of RMTs	10	20	20	10

4.2. Dynamic Performance Analysis

The dynamic performance of each workstation and product in both the PI-RRCF and ISPI-RRCF capacity control systems while facing stochastic demands are shown in Figures 7–10. The dynamic optimization values of both the PI and ISPI tracking control parameters with the single neuron are given in Figure 9.

In Figure 7, the blue and red lines represent the WIP levels controlled by PI-RRCF and ISPI-RRC, respectively. In workstation 1, the initial WIP constantly increased with the orders flowing into the workstation at the initial stage, which could cause a bottleneck. This phenomenon can be explained—in the first few hours, the RMTs were not completely reconfigured and assigned to workstations due to reconfiguration delays and transportation delays (cf. Figure 8). However, the ISPI-RRCF control system showed a quicker response than that of the PI-RRCF system in terms of assigning RMTs to the workstation in the case of a bottleneck. After 20 h, the WIP levels were kept in the vicinity of the planned values for both the ISPI-RRCF and PI-RRCF control systems. Nonetheless, the former showed better dynamic performance with lower overshoots and shorter settling times. In contrast to workstation 1, the initial WIP levels in the other workstations were lower than or equal to their respective planned values. As the order outputs were higher than the input rates, the WIP levels decreased in the first few hours. Later, with more orders flowing through these workstations, the WIP started to increase and approach the planned levels. However, due to the lag effect caused by delays and the accumulation of integration, PI-RRCF had a higher overshoot and longer settling times. This indicated that, compared with the previous PI-RRCF, the proposed ISPI-RRCF could effectively improve the transient performance to avoid a high overshoot, which represented the bottleneck level and unbalanced capacity distribution. This greatly improved the productivity and decreased the production costs.

Figure 8 shows the distribution of RMTs of each workstation in the capacity control processes, which shows that the response in the ISPI-RRCF control system was quicker than that of the PI-RRCF system in the assignment of RMTs to the required workstations. With the orders flowing to the next workstations, two RMTs, one RMT, and one RMT were, respectively, assigned to workstations 2, 3, and 4 at the 9th, 14th, and 15th hours, respectively. However, in the PI-RRCF system, five RMTs, one RMT, one RMT, and one RMT were, respectively, assigned to workstations 1, 2, 3, and 4 at the 5th, 9th, 27th, and 35th hours, respectively. Additionally, the ISPI-RRCF showed a bit less utilization of RMTs while facing quickly changing customer demand, which could reduce the production costs from the machine tools. Therefore, this indicates that the ISPI-RRCF could predict

possible bottlenecks and assign enough RMTs to balance the capacity distribution by using the customized flexibility of RMTs. This further illustrates the quicker response in the ISPI-RRCF control system for effectively deducing high overshoots and avoiding bottleneck problems, which highly decreased the production costs and improved the dynamic performance.

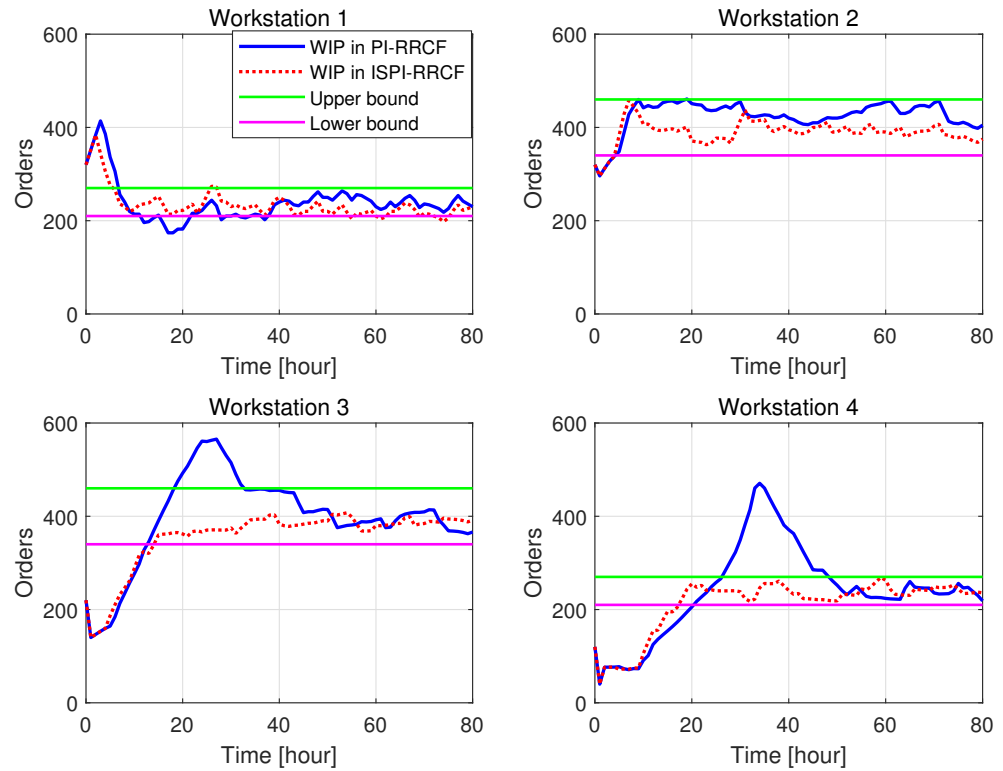


Figure 7. WIP levels of workstations for stochastic demands.

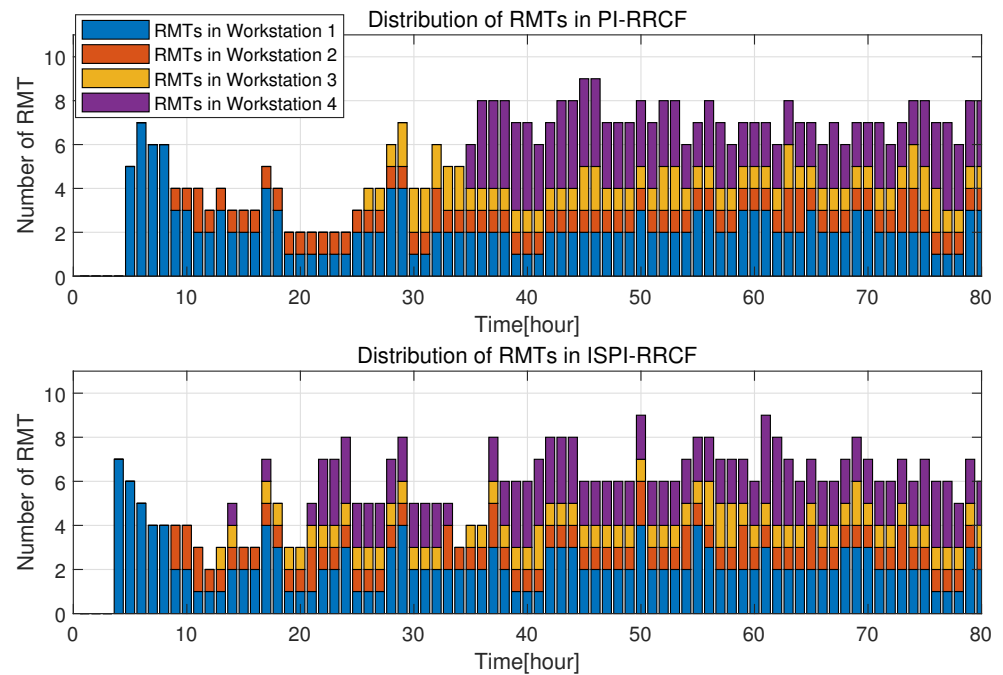


Figure 8. Distribution of RMTs for stochastic demands.

For the tracking control parameter values, Figure 9 shows the dynamic optimization results obtained by using the single neuron in both the PI-RRCF and ISPI-RRCF capacity control processes. With the decoupling control, each workstation was an independent SISO system. Therefore, the parameter optimization was relatively independent in both the PI-RRCF and ISPI-RRCF systems. However, compared with Figure 8, the curves for the KP (i.e., C_i^0) and KI (i.e., C_i^1) in ISPI-RRCF showed relatively stable behaviors after 10 h, while the PI-RRCF took a longer time. The KI values in all workstations went toward 0 to avoid high overshoots when the error was over set threshold in the ISPI-RRCF control system. However, the KI values were not zeros in the PI-RRCF system, which explained one of the reasons for the high overshoots. From the overall settings, these values had relatively quicker updating in ISPI-RRCF in order to solve bottlenecks, and they had relatively stable settings when facing bounded stochastic input rates. This illustrated the effectiveness of the proposed adaptive algorithm based on a single neuron with supervised Hebb learning. On the other hand, this could also imply the better dynamic and robust performances in the ISPI-RRCF control system.

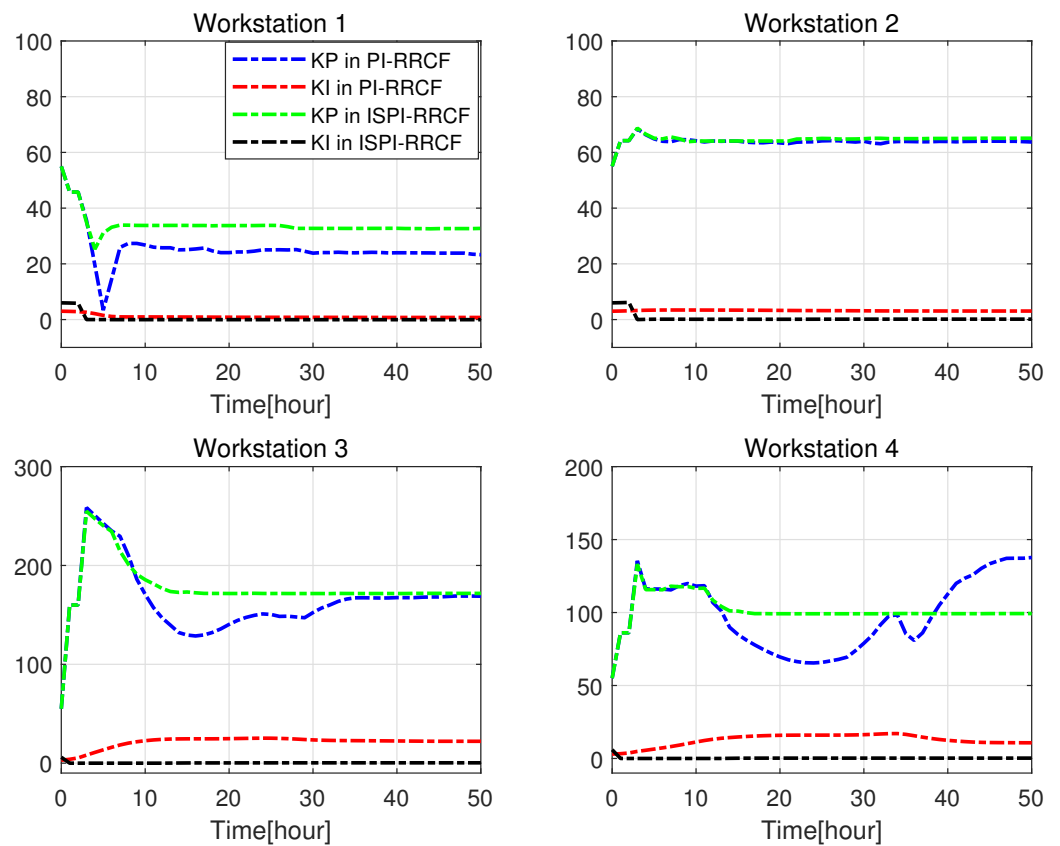


Figure 9. Value of the tracking controller’s parameters.

Unlike the performance analysis in the workstations, the input and output rates of each product were not independent, which caused dynamic changes in the workstations’ productivity. When facing stochastic demands, the input rates of each product were the same in both control systems, as shown with the black lines in Figure 10. The blue and red lines represent the product output rates in the PI-RRCF and ISPI-RRCF control systems. Products 1, 2, and 3 were produced starting from the first, second, and first workstations and were finished at the third, fourth, and fourth workstations, respectively. The output rate of each product was produced by the DMTs at the beginning. With the additional RMTs assigned to the later two workstations, the output rates were quickly increased around the input rate in 20 h in the ISPI-RRCF system. However, the PI-RRCF system took a longer time. Additionally, the output rates in ISPI-RRCF were around the input

rate for most of the time, which showed that there was greater customer satisfaction in this system. In summary, when facing stochastic customer demands, both control systems were able to provide the required output products, while the proposed ISPI-RRCF system still showed better dynamic performance with a quicker response for satisfying customers' stochastic demands.

Considering the transient performance in the above figures, it was concluded that both control systems could deal with stochastic demands to guarantee that the WIP of workstations was kept in the vicinity of the desired level and that the output rate of the products was kept close to the input rates. However, the proposed adaptive ISPI-RRCF tracking capacity control system showed better behaviors with a quicker response and lower overshoot. This indicated that the control system could significantly avoid serious bottlenecks and quickly balance the capacity distribution to improve the productivity and decrease the inventory and production costs, which also illustrated the effectiveness of the proposed ISPI-RRCF method.

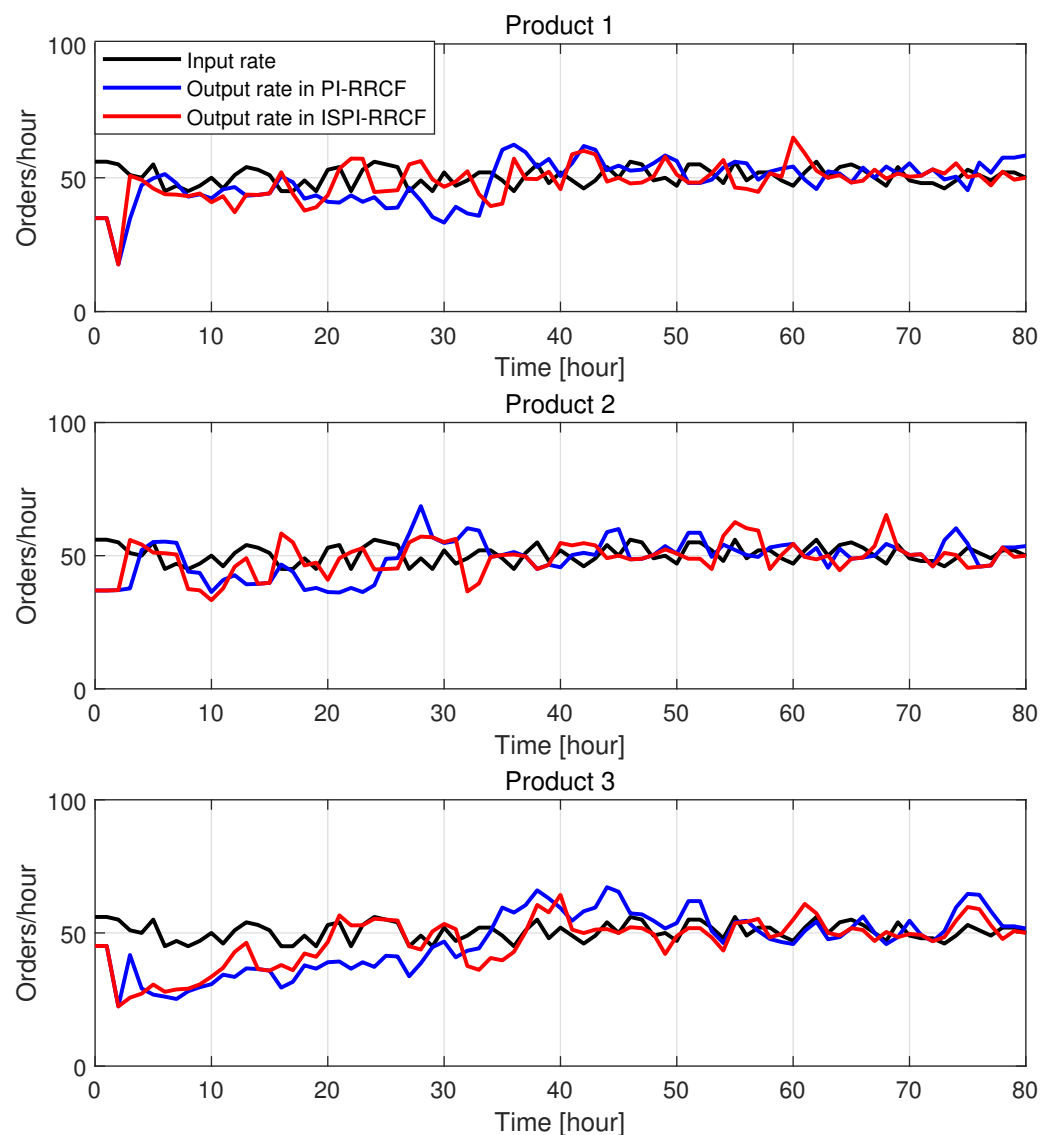


Figure 10. Dynamic performance of the products.

4.3. Robustness Analysis

Stochastic customer demands and different types of products were considered when measuring and analyzing the robustness of the capacity control systems. In this part, robustness was defined as the mean and standard deviation of the output variables. The dis-

tribution of the error between the planned and current WIP at each workstation is given in Figure 11. The blue and red error bars are the distributions of errors in the PI-RRCF and ISPI-RRCF capacity control systems. These showed that the distributions in the red bars of all workstations were highly concentrated, with smaller mean values and standard deviations than those of the blue bars, which indicated that the WIP values of the workstations were distributed closer to the desired levels in the ISPI-RRCF system, with a higher robustness. Additionally, the red error bars were distributed over zero, which meant that the WIP levels of the workstations were lower than the planned level in most cases. This illustrated the lower possibility of bottleneck occurrence in this control system.

Figure 12 shows the distribution of products while considering the input and output rates. The black error bars present the distribution of order input rates. The blue and red error bars in the PI-RRCF and ISPI-RRCF were relatively broad, but the latter distribution was still relatively concentrated. This showed that the robustness when considering the order output rate of products in the ISPI-RRCF system was still higher than that in the PI-RRCF system.

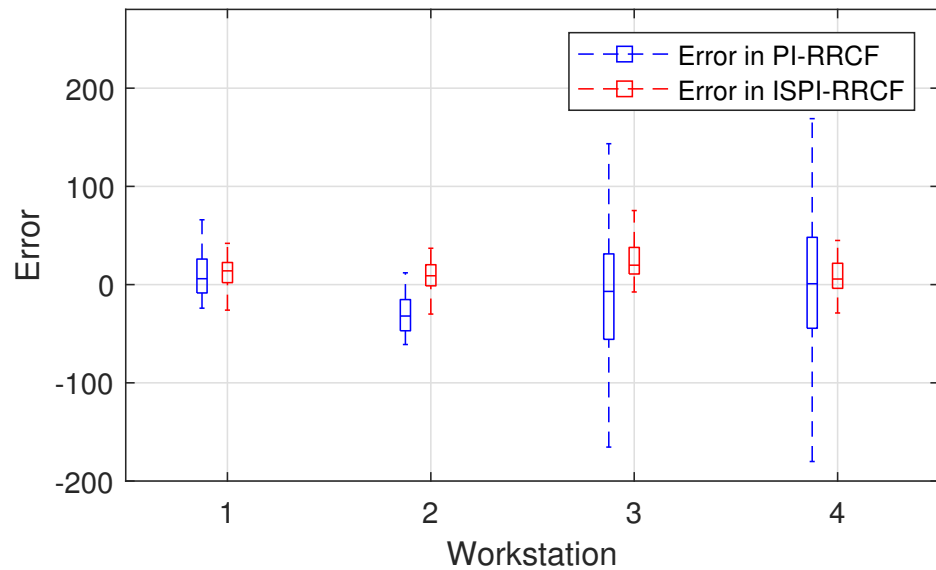


Figure 11. Error distributions between the planned and current WIP of the workstations.

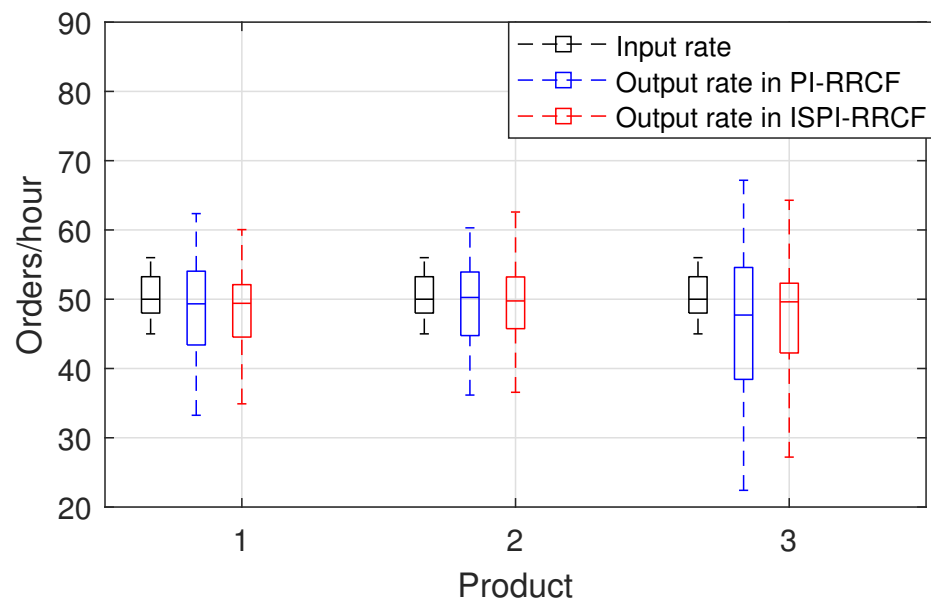


Figure 12. Input and output rate distributions of the products.

The overall statistics of the transient and robustness performance in both the ISPI-RRCF and PI-RRCF control systems are summarized in Table 3. The mean number of RMTs (MRMT) and standard deviation of RMTs (SDRMT) at each workstation were close in the ISPI-RRCF and PI-RRCF control systems. Nonetheless, the mean value of the absolute error (MAE) between the desired and actual WIP, as well as the standard deviation of the absolute error (SDAE), were smaller in the ISPI-RRCF system, which further indicated the higher robustness of this capacity control system. The transient performance when considering the overshoot and settling times of these two control systems was also collected. This further showed that the dynamic performance in the ISPI-RRCF system was better than that in the PI-RRCF system, with smaller overshoots and shorter settling times.

Table 3. Statistics of the capacity control systems.

Number of the Workstation	1	2	3	4
MRMT in PI-RRCF	2.22	0.99	0.87	1.65
MRMT in ISPI-RRCF	2.23	1.01	0.87	1.66
SDRMT in PI-RRCF	1.22	0.41	0.69	1.52
SDRMT in ISPI-RRCF	1.17	0.52	0.49	1.11
MAE in PI-RRCF	18.85	34.62	51.97	60.90
MAE in ISPI-RRCF	17.24	13.25	26.65	21.55
SDAE in PI-RRCF	16.28	16.37	49.79	65.72
SDAE in ISPI-RRCF	10.43	10.46	28.89	34.74
Overshoots in PI-RRCF	0.72	0.15	0.41	0.96
Overshoots in ISPI-RRCF	0.60	0.14	0.02	0.12
Setting time in PI-RRCF	21	5	32	48
Setting time in ISPI-RRCF	6	5	13	18

In summary, for the capacity control of the complex job shop system with transportation delays, reconfiguration delays, and stochastic demand, the key system performance indexes and control performance indexes are discussed. The system performance indexes were represented by the WIP of the workstations and the output rate of the products, while the control performance indexes were represented by the transients and robustness. The performance of the proposed adaptive ISPI-RRCF and PI-RRCF control systems is compared and analyzed in this section. The system performance indexes showed that both control systems could keep the WIP and product output rate at the desired value to ensure productivity and satisfy customer demands. However, ISPI-RRCF had better transient and robustness performance in terms of its lower overshoots, shorter settling times, and smaller means and standard deviations. This indicated that the proposed algorithm could greatly improve the performance to avoid serious bottlenecks and balance the capacity distribution for high productivity, low costs, and high customer satisfaction.

5. Conclusions

This paper focused on the adaptive tracking capacity control of complex job shops. Considering stochastic customer demands, an improved ISPI-RRCF adaptive capacity control method was proposed to enhance the transient and robustness performance. Considering the customized flexibility of RMTs and the complexity of job shops, including stochastic customer demands, reconfiguration delays of RMTs, and transportation delays between workstations, a funnel-based mathematical model was introduced for the capacity controller design. Based on this model, an operator-based capacity controller was designed, which included a decoupling controller for the MIMO system and, later, a local ISPI-RRCF capacity controller for decoupled SISO systems. In particular, the local ISPI-RRCF controller was designed by including an RRCF controller and ISPI tracking controller, where the parameters were dynamically optimized by a single neuron based on the supervised Hebb learning algorithm. The stability of the closed-loop system was theoretically proven based on the Lipschitz norm. Finally, a case study for the capacity control of a job shop system was implemented in a simulation. The transient and robustness performance of the

proposed ISPI-RRCF control system was analyzed and compared with that of a previous PI-RRCF control system. The results showed that when considering the system performance indexes, both the proposed ISPI-RRCF and the previous PI-RRCF capacity control systems could keep the WIP of all workstations in the vicinity of the planned levels and could keep the output rate of the products close to the input rates. However, for the control performance indexes, the proposed ISPI-RRCF system had a better transient performance with smaller overshoots and shorter settling times, as well as better robustness, with a smaller MAE and SDAE. Therefore, the effectiveness of the proposed adaptive ISPI-RRCF capacity control algorithm could be proven due to the avoidance of serious bottlenecks and the balancing of capacity distribution problems. This research also provides new opportunities for manufacturers for higher productivity, lower costs, and greater customer satisfaction when facing challenges from quickly changing markets, new technological revolutions, and sustainable manufacturing.

Author Contributions: Conceptualization, P.L.; methodology, P.L.; software, P.L.; validation, P.L. and Q.Z.; investigation, P.L., A.W. and J.P.; writing—original draft preparation, P.L. and Q.Z.; writing—review and editing, S.W.; visualization, A.W.; supervision, J.P.; project administration, P.L. All authors have read and agreed to the published version of the manuscript.

Funding: This research was partially supported by the National Key Research and Development Program of China (grant number 2020YFB1712403) and the Key Scientific and Technological Project of Henan Province (grant numbers 212102210380 and 212102210080).

Institutional Review Board Statement: Not applicable.

Informed Consent Statement: Not applicable.

Data Availability Statement: Not applicable.

Conflicts of Interest: The authors declare no conflicts of interest.

References

1. Scholz-Reiter, B.; Freitag, M.; Schmieder, A. Modelling and control of production systems based on nonlinear dynamics theory. *CIRP Ann.* **2002**, *51*, 375–378. [[CrossRef](#)]
2. Alkan, B.; Vera, D.A.; Ahmad, M.; Ahmad, B.; Harrison, R. Complexity in manufacturing systems and its measures: A literature review. *Eur. J. Ind. Eng.* **2018**, *12*, 116–150. [[CrossRef](#)]
3. Thüerer, M.; Stevenson, M.; Land, M.J.; Fredendall, L.D. On the combined effect of due date setting, order release, and output control: An assessment by simulation. *Int. J. Prod. Res.* **2019**, *57*, 1741–1755. [[CrossRef](#)]
4. Stastny, J.; Skorpil, V.; Balogh, Z.; Klein, R. Job Shop Scheduling Problem Optimization by Means of Graph-Based Algorithm. *Appl. Sci.* **2021**, *11*, 1921. [[CrossRef](#)]
5. Liu, P.; Zhang, Q.; Pannek, J. Development of operator theory in the capacity adjustment of job shop manufacturing systems. *Appl. Sci.* **2019**, *9*, 2249. [[CrossRef](#)]
6. Zhang, Q.; Liu, P.; Chen, Y.; Deng, Q.; Pannek, J. An improved event-triggered predictive control for capacity adjustment in reconfigurable job-shops. *Int. J. Prod. Res.* **2022**, 1–18. [[CrossRef](#)]
7. Karimi, H.R.; Duffie, N.A.; Dashkovskiy, S. Local capacity h_∞ control for production networks of autonomous work systems with time-varying delays. *IEEE Trans. Autom. Sci. Eng.* **2010**, *7*, 849–857. [[CrossRef](#)]
8. Landers, R.G.; Min, B.K.; Koren, Y. Reconfigurable machine tools. *CIRP Ann. Manuf. Technol.* **2001**, *50*, 269–274. [[CrossRef](#)]
9. Scholz-Reiter, B.; Lappe, D.; Grundstein, S. Capacity adjustment based on reconfigurable machine tools—Harmonising throughput time in job-shop manufacturing. *CIRP Ann.* **2015**, *64*, 403–406. [[CrossRef](#)]
10. Zhang, Q.; Liu, P.; Pannek, J. Modeling and predictive capacity adjustment for job shop systems with RMTs. In Proceedings of 25th Mediterranean Conference on Control and Automation (MED), Valletta, Malta, 3–6 July 2017.
11. Zhong, R.Y.; Xu, X.; Klotz, E.; Newman, S.T. Intelligent manufacturing in the context of industry 4.0: A review. *Engineering* **2017**, *3*, 616–630. [[CrossRef](#)]
12. Kim, J.H.; Duffie, N.A. Backlog control design for a closed loop PPC system. *CIRP Ann.* **2004**, *53*, 357–360. [[CrossRef](#)]
13. Kim, J.H.; Duffie, N.A. Performance of coupled closed-loop workstation capacity controls in a multi-workstation production system. *CIRP Ann.* **2006**, *55*, 449–452. [[CrossRef](#)]
14. Ang, K.H.; Chong, G.; Li, Y. PID control system analysis, design, and technology. *IEEE Trans. Control Syst. Technol.* **2005**, *13*, 559–576.
15. Chen, G.; Han, Z. Robust right coprime factorization and robust stabilization of nonlinear feedback control systems. *IEEE Trans. Automat. Control* **1998**, *43*, 1505–1509. [[CrossRef](#)]

16. Deng, M.; Inoue, A.; Ishikawa, K. Operator-based nonlinear feedback control design using robust right coprime factorization. *IEEE Trans. Autom. Control.* **2006**, *51*, 645–648. [[CrossRef](#)]
17. Xu, Y.; Deng, M. Particle Filter Design for Robust Nonlinear Control System of Uncertain Heat Exchange Process with Sensor Noise and Communication Time Delay. *Appl. Sci.* **2022**, *12*, 2495. [[CrossRef](#)]
18. Bi, S.; Deng, M.; Xiao, Y. Robust stability and tracking for operator-based nonlinear uncertain systems. *IEEE Trans. Autom. Sci. Eng.* **2014**, *12*, 1059–1066. [[CrossRef](#)]
19. Deng, M.; Wang, A. Robust non-linear control design to an ionic polymer metal composite with hysteresis using operator-based approach. *IET Control Theory Appl.* **2012**, *6*, 2667–2675. [[CrossRef](#)]
20. Bu, N.; Pang, J.; Deng, M. Robust fault tolerant tracking control for the multi-joint manipulator based on operator theory. *J. Frankl. Inst.* **2020**, *357*, 2696–2714. [[CrossRef](#)]
21. Wen, S.; Deng, M.; Bi, S.; Wang, D. Operator-based robust nonlinear control and its realization for a multi-tank process by using a distributed control system. *Trans. Inst. Meas. Control* **2012**, *34*, 891–902. [[CrossRef](#)]
22. Gharib, M.R.; Koochi, A.; Ghorbani, M. Path tracking control of electromechanical micro-positioner by considering control effort of the system. *Proc. Inst. Mech. Eng. Part I J. Syst. Control. Eng.* **2021**, *235*, 984–991. [[CrossRef](#)]
23. Salehi Kolahi, M.R.; Gharib, M.R.; Heydari, A. Design of a non-singular fast terminal sliding mode control for second-order nonlinear systems with compound disturbance. *Proc. Inst. Mech. Eng. Part C J. Mech. Eng. Sci.* **2021**, *235*, 7343–7352. [[CrossRef](#)]
24. Nguyen, M.H.; Dao, H.V.; Ahn, K.K. Adaptive robust position control of Electro-Hydraulic servo systems with large uncertainties and disturbances. *Appl. Sci.* **2022**, *12*, 794. [[CrossRef](#)]
25. Ruan, W.; Dong, Q.; Zhang, X.; Li, Z. Friction compensation control of electromechanical actuator based on Neural Network Adaptive Sliding Mode. *Sensors* **2021**, *21*, 1508. [[CrossRef](#)] [[PubMed](#)]
26. Sidhu, A.S.; Singh, S.; Kumar, R.; Pimenov, D.Y.; Giasin, K. Prioritizing energy-intensive machining operations and gauging the influence of electric parameters: An industrial case study. *Energies* **2021**, *14*, 4761. [[CrossRef](#)]
27. Lödging, H. A manufacturing control model. *Int. J. Prod. Res.* **2012**, *50*, 6311–6328. [[CrossRef](#)]
28. Zhang, Q.; Freitag, M.; Pannek, J. Stability of Predictive Control in Job Shop System with Reconfigurable Machine Tools for Capacity Adjustment. *Logist. Res.* **2019**, *12*, 3.
29. Zhang, Q.; Liu, P.; Pannek, J. Combining MPC and integer operators for capacity adjustment in job-shop systems with RMTs. *Int. J. Prod. Res.* **2019**, *57*, 2498–2513. [[CrossRef](#)]
30. Liu, P.; Zhang, Q.; Pannek, J. Evaluation of Control Approaches for Capacity Adjustment in Job Shop Systems. *IFAC-PapersOnLine* **2019**, *52*, 1966–1971. [[CrossRef](#)]
31. Liu, P.; Zhang, Q.; Wang, A.; Song, J.; Li, D.; Yan, Y.; Yang, L. Machinery-oriented Capacity Control for Complex Industrial Manufacturing Processes. In Proceedings of the 2021 International Conference on Advanced Mechatronic Systems (ICAMechS), Tokyo, Japan, 9–12 December 2021.
32. Xiang, Z.; Shao, X.; Wu, H.; Ji, D.; Yu, F.; Li, Y. An adaptive integral separated proportional–integral controller based strategy for particle swarm optimization. *Knowl.-Based Syst.* **2020**, *195*, 105696. [[CrossRef](#)]
33. Joseph, S.B.; Dada, E.G.; Abidemi, A.; Oyewola, D.O.; Khammas, B.M. Metaheuristic algorithms for PID controller parameters tuning: Review, approaches and open problems. *Heliyon* **2022**, *8*, e09399. [[CrossRef](#)]
34. Li, W.; Hori, Y. Vibration suppression using single neuron-based PI fuzzy controller and fractional-order disturbance observer. *IEEE Trans. Ind. Electron.* **2007**, *54*, 117–126. [[CrossRef](#)]
35. Liu, P.; Chinges, U.; Zhang, Q.; Pannek, J. Capacity control in disturbed and time-delayed job shop manufacturing systems with RMTs. *IFAC-PapersOnLine* **2018**, *51*, 807–812. [[CrossRef](#)]

Disclaimer/Publisher’s Note: The statements, opinions and data contained in all publications are solely those of the individual author(s) and contributor(s) and not of MDPI and/or the editor(s). MDPI and/or the editor(s) disclaim responsibility for any injury to people or property resulting from any ideas, methods, instructions or products referred to in the content.